

MIT Open Access Articles

*Were the May 2012 Emilia-Romagna earthquakes induced?
A coupled flow-geomechanics modeling assessment*

The MIT Faculty has made this article openly available. *Please share* how this access benefits you. Your story matters.

Citation: Juanes, R., B. Jha, B. H. Hager, et al. "Were the May 2012 Emilia-Romagna Earthquakes Induced? A Coupled Flow-Geomechanics Modeling Assessment." *Geophysical Research Letters*, vol. 43, no. 13, 2016, pp. 6891-6897. © 2016 American Geophysical Union.

As Published: <http://dx.doi.org/10.1002/2016GL069284>

Publisher: American Geophysical Union (AGU)/Wiley

Persistent URL: <http://hdl.handle.net/1721.1/106543>

Version: Final published version: final published article, as it appeared in a journal, conference proceedings, or other formally published context

Terms of Use: Article is made available in accordance with the publisher's policy and may be subject to US copyright law. Please refer to the publisher's site for terms of use.





RESEARCH LETTER

10.1002/2016GL069284

Key Points:

- Coupled flow-geomechanics modeling permits integration of geologic, seismotectonic, well log, fluid pressure/flow rate, and geodetic data
- We use geomechanics models to assess whether injected and produced fluids may have induced two $\sim M6$ May 2012 earthquakes in northern Italy
- Our study illustrates a promising approach for assessing and managing hazard associated with induced seismicity

Supporting Information:

- Supporting Information S1
- Movie S1
- Movie S2

Correspondence to:

R. Juanes,
juanes@mit.edu

Citation:

Juanes, R., B. Jha, B. H. Hager, J. H. Shaw, A. Plesch, L. Astiz, J. H. Dieterich, and C. Frohlich (2016), Were the May 2012 Emilia-Romagna earthquakes induced? A coupled flow-geomechanics modeling assessment, *Geophys. Res. Lett.*, *43*, 6891–6897, doi:10.1002/2016GL069284.

Received 20 APR 2016

Accepted 27 JUN 2016

Accepted article online 2 JUL 2016

Published online 8 JUL 2016

Were the May 2012 Emilia-Romagna earthquakes induced? A coupled flow-geomechanics modeling assessment

R. Juanes^{1,2}, B. Jha^{1,3}, B. H. Hager², J. H. Shaw⁴, A. Plesch⁴, L. Astiz^{5,6}, J. H. Dieterich⁷, and C. Frohlich⁸

¹Department of Civil and Environmental Engineering, Massachusetts Institute of Technology, Cambridge, Massachusetts, USA, ²Department of Earth, Atmospheric and Planetary Sciences, Massachusetts Institute of Technology, Cambridge, Massachusetts, USA, ³Now at Department of Chemical Engineering and Materials Science, University of Southern California, Los Angeles, California, USA, ⁴Department of Earth and Planetary Sciences, Harvard University, Cambridge, Massachusetts, USA, ⁵Institute of Geophysics and Planetary Physics, University of California, San Diego, La Jolla, California, USA, ⁶Now at Earth Sciences Division, National Science Foundation, Washington, District of Columbia, USA, ⁷Department of Earth Sciences, University of California, Riverside, California, USA, ⁸Jackson School of Geosciences, University of Texas at Austin, Austin, Texas, USA

Abstract Seismicity induced by fluid injection and withdrawal has emerged as a central element of the scientific discussion around subsurface technologies that tap into water and energy resources. Here we present the application of coupled flow-geomechanics simulation technology to the post mortem analysis of a sequence of damaging earthquakes ($M_w = 6.0$ and 5.8) in May 2012 near the Cavone oil field, in northern Italy. This sequence raised the question of whether these earthquakes might have been triggered by activities due to oil and gas production. Our analysis strongly suggests that the combined effects of fluid production and injection from the Cavone field were not a driver for the observed seismicity. More generally, our study illustrates that computational modeling of coupled flow and geomechanics permits the integration of geologic, seismotectonic, well log, fluid pressure and flow rate, and geodetic data and provides a promising approach for assessing and managing hazards associated with induced seismicity.

1. Introduction

Earthquakes are a paradigmatic example of our limited ability to make predictions in the geosciences. Despite their frequent occurrence and devastating consequences and the extensive body of knowledge accumulated over time—both in terms of prevalent geologic settings and physical principles [e.g., Scholz, 2002; Kawamura *et al.*, 2012]—natural earthquakes remain unpredictable.

The recent rise in seismicity in intraplate regions like the Continental United States, however, is associated with anthropogenic activities. Much of the evidence of triggered or induced seismicity is related to subsurface disposal of wastewater from mature oil fields or caused as a result of unconventional oil and gas extraction and coproduced water reinjection [Frohlich, 2012; Ellsworth, 2013; Keranen *et al.*, 2013, 2014; van der Elst *et al.*, 2013; Weingarten *et al.*, 2015; Improta *et al.*, 2015]. While the potential for subsurface fluid injection and extraction to trigger earthquakes has long been recognized [e.g., Raleigh *et al.*, 1976; Segall, 1989], the sharp increase in the extent and vigor of induced seismicity calls for much deeper understanding than is currently available [e.g., National Research Council, 2013; Guglielmi *et al.*, 2015; Hornbach *et al.*, 2015].

Here we contend that induced earthquakes may be better understood, modeled and forecast than natural earthquakes, and—eventually—perhaps managed. The reason is twofold. First, it is possible to acquire a relatively dense set of subsurface measurements that provide detailed knowledge of the geologic structure before exploitation, and to deploy a monitoring program that quantifies changes within that structure, including bottom hole pressures, water cuts and gas-oil ratios, surface deformation, and microseismicity. Second, the injection and extraction of fluids are causally linked to changes in fluid pressures and in the tensor stress state of the subsurface. This linkage can be quantified by mathematical models that describe the coupling between flow through rocks and deformation of those rocks in the presence of fractures and faults.

We propose that geologically realistic computational models of coupled reservoir flow and geomechanics permit the integration of seismic, well log, fluid pressure and flow rate, and other, e.g., geodetic, data in a way that enables quantitative assessments of the likelihood of induced seismicity, strategies that prevent

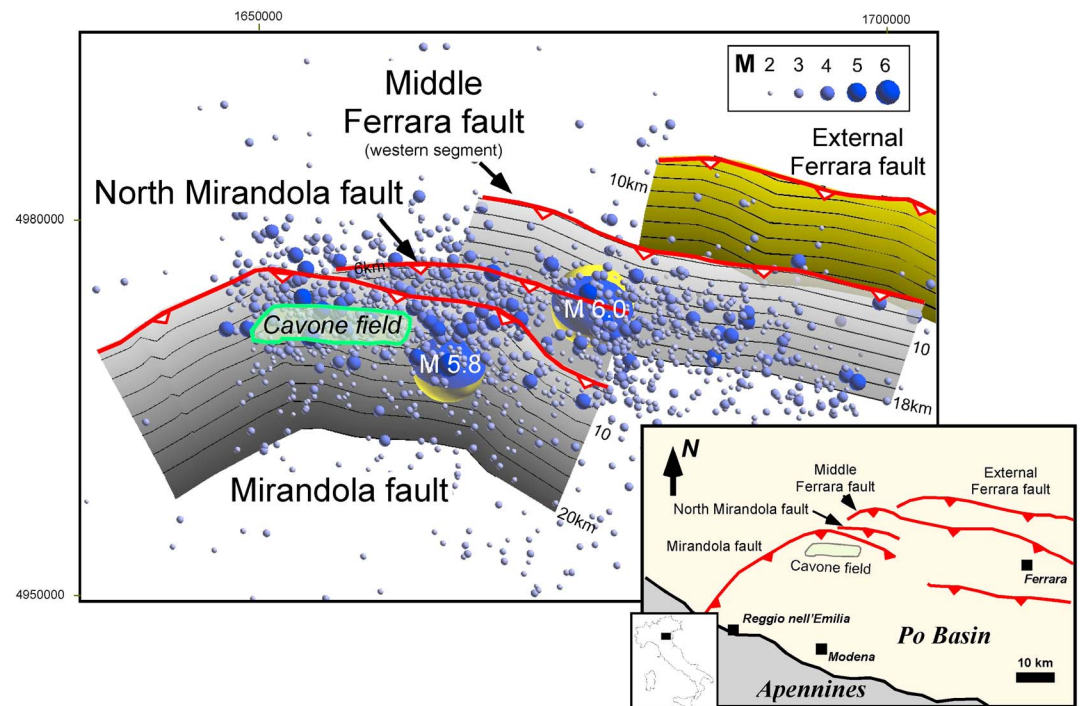


Figure 1. Main faults in the Cavone area and May 2012 earthquake hypocenters. Map showing location of the Cavone oil field, epicenters with focal mechanisms of the two largest 2012 Emilia-Romagna earthquakes, epicenters from the INGV earthquake catalog (January 2011 to February 2013), and principal thrust faults. Inset shows faults that comprise the Ferrarese-Romagnolo arc in the Po basin.

it, or remediation programs that mitigate it. Naturally, this would have important social, economic, and regulatory consequences.

We illustrate the potential of predictive computational models of likelihood of induced seismicity with a detailed case study exploring potential connections between the May 2012 Emilia-Romagna sequence in northern Italy and operations in the nearby Cavone oil field. Our analysis addresses the question of whether this earthquake sequence might have been triggered by fluid extraction and injection and, if it is not, whether it is plausible that future reservoir operations could trigger other seismic events.

2. Tectonic Framework

In Italy's history there have been numerous damaging earthquakes, including events in 1857, 1908, and 1915 with 11,000; 72,000; and 32,000 fatalities, respectively. A notable feature of the region's strong earthquakes is that they are broadly distributed across a complex network of faults in Italy rather than concentrated along a single well-developed fault zone. The May 2012 Emilia-Romagna earthquake sequence, which caused about 25 fatalities, occurred in the eastern Po Plain, a region situated between the Apennine mountains (to the south) and the Alps (to the north) known to be seismically active [Burrato *et al.*, 2003]. Historically, over 100 earthquakes have been felt in the city of Ferrara, with 26 of those events having estimated magnitude $M_e \geq 4.0$ (Istituto Nazionale di Geofisica e Vulcanologia, 2016, <http://storing.ingv.it/cfti.4med/> (consulted February 2, 2016)) and a largest recorded event prior to the May 2012 sequence—the 1570 Ferrara earthquake—having estimated magnitude $M_e 5.5$.

The Cavone oil field is located in the Apennine foreland, in an area known as the Ferrarese-Romagnolo arc (Figure 1a). Structures in this area are dominated by deep-seated reverse faults that are “blind,” that is, which do not reach the surface and have displacements that decrease upward into the cores of the overlying fault-related folds [Stein and Yeats, 1989; Shaw and Suppe, 1996; Ciaccio and Chiarabba, 2002; Bonini, 2013]. This structural style is manifest in the Cavone field, which consists of a north vergent fault-propagation fold [Suppe and Medwedeff, 1990; Shaw *et al.*, 2005] underlain by the steeply south dipping Mirandola thrust (Figure 1b).

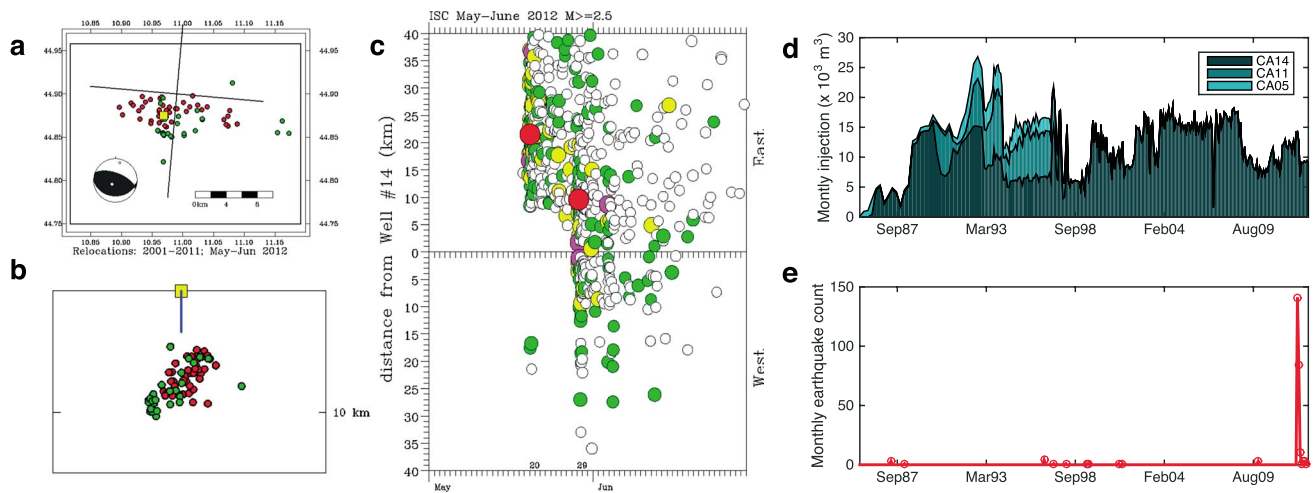


Figure 2. Seismicity near the Cavone #14 water injection well. (a) Map of relocations for selected earthquakes (circles) around Cavone well #14 (yellow square). Green circles: 28 events occurring 2001 to 2011; red circles: 41 events occurring May–June 2012. Plotted focal mechanism for 20 May 2012 earthquake is from the Global GCMT catalog. Thick lines indicate orientations of cross sections. (b) West facing cross section for selected relocated earthquakes (circles) around Cavone well #14 (yellow square and blue line). Green circles: 28 events occurring 2001 to 2011; red circles: 41 events occurring May–June 2012. Note that hypocentral depths for both groups range mostly between 5 km and 10 km. (c) Space-time plot of epicenters during May–June 2012 (circles; plot includes events with $M < 2.5$). Vertical axis shows distance between epicenters and Cavone well #14; (top) earthquakes east of well; (bottom) earthquakes west of well. Colors/sizes indicate reported magnitudes; white: $M < 3$; green: $3 < M < 4$; yellow: $4 < M < 5$; pink: $M > 5$; and red: 20 and 29 May 2012 earthquakes. Plotted epicenters are as reported by the International Seismological Centre, which combines information reported by various organizations, including INGV. (d) Monthly injection volumes at the three water injectors in the Cavone field, from February 1986 to December 2012. Injectors CA5 and CA11 were shut in October 1997. (e) Monthly count of earthquakes with $M > 2.5$ at a distance < 10 km from the Cavone #14 well, also during the period February 1986 through December 2012. The spike corresponds to the May–June 2012 seismicity.

The 2012 Emilia-Romagna earthquake sequence comprised two main events: the 20 May 2012 M_w 6.0, and 29 May M_w 5.8 events. There are clear indications—based on its hypocentral depth and aftershock distribution—that the 20 May earthquake sourced on the western segment of the Middle Ferrara fault [Pezzo *et al.*, 2013] and that the 29 May earthquake occurred about 10 km to the southwest of the 20 May event. Our locations of the 29 May earthquake and its aftershocks, in agreement with those reported by the Istituto Nazionale di Geofisica e Vulcanologia (INGV) [Scognamiglio *et al.*, 2012], suggest it was sourced by the Mirandola fault, which bounds the Cavone field from the north (Figure 1b). Thus, we conclude that the 20 and 29 May earthquakes occurred on separate, en echelon blind thrust faults.

3. Seismotectonic Analysis

To investigate the apparent relation between earthquake activity and oil field reservoir operations, we analyze regional seismicity before and after the May 2012 earthquakes, with an emphasis on activity near the Cavone well #14, which has been injecting water into the subsurface since 1986. We relocated a select group of events near Cavone well #14 occurring between 2001 and June 2012, which have been particularly well recorded by a network of seismograph stations managed by the Operator (see supporting information). The 28 relocated hypocenters that occurred years prior to the 2012 sequence (green circles in Figure 2a) have focal depths between 4.6 km and 10.3 km and are located along a southward-dipping plane approximately coincident with one nodal plane of the 20 May 2012 earthquake (Figure 2b).

The Emilia-Romagna earthquake sequence has properties of a cascading series of foreshocks and aftershocks common with tectonic earthquakes (Figure 2c) (see supporting information). Taken together, seismological [Cesca *et al.*, 2013; Ganas *et al.*, 2012; Piccinini *et al.*, 2012] and geodetic [Pezzo *et al.*, 2013] analyses of the coseismic and immediate postseismic displacements from the principal events indicate a complex source for the 20 May earthquake, and likely static triggering of the 29 May event [Cesca *et al.*, 2013; Pezzo *et al.*, 2013]. However, and despite a lack of correlation between water injection and seismicity (Figures 2d and 2e), the location of Cavone well #14 in the vicinity of the 29 May earthquake rupture and aftershock zone highlights the need for a mechanistic analysis that evaluates the potential link between pressure variations from fluid injection and production and stressing of the Mirandola fault.

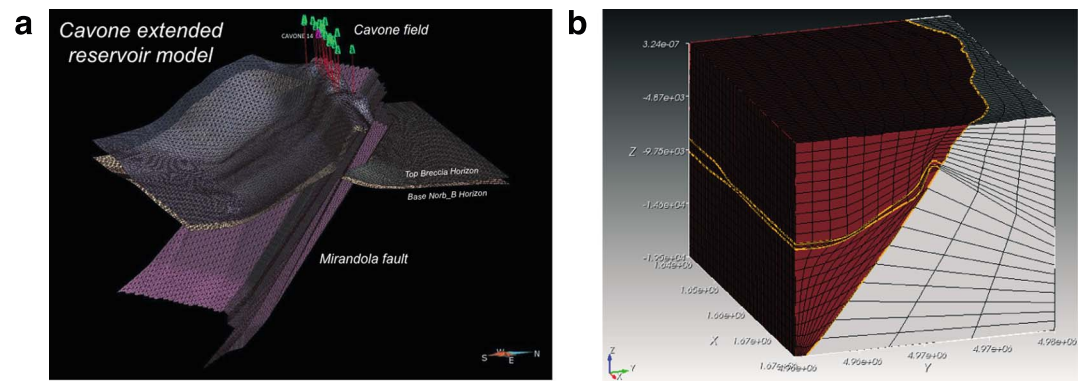


Figure 3. Structural model and coupled flow-geomechanics model. (a) Perspective view of the extended Cavone reservoir model, showing the upper and lower reservoir horizons and the Mirandola fault. (b) Geomechanics grid constructed using the top and bottom reservoir surfaces and the Mirandola fault. Red color indicates the hanging wall and light color the foot wall. The coordinate system is such that the x axis is easting, the y axis is northing, and the z axis is elevation in meters.

4. Results From Coupled Flow and Geomechanics Modeling

To address this question, we developed a new reservoir model that combines an accurate representation of the geology with fidelity in the description of the coupled multiphysics at play. We include the major stratigraphic and structural elements in the region, with particular emphasis on the precise structural relationships between the Mirandola fault and the reservoir units. In this way, we are able to examine, via coupling of flow and geomechanics modeling, how fluid pressure changes from reservoir operations affects stresses acting on the fault. Fault and stratigraphic horizons were mapped using a regional grid of migrated seismic reflection profiles and well tops from the Cavone field. Seismic reflection data were converted to depth using a velocity model developed from sonic logs. Stratigraphic horizons and faults are first represented as triangulated surfaces (Figure 3a), and these representations serve as the basis for developing a computational mesh of hexahedral elements (Figure 3b) (see supporting information).

We simulate the interplay between fluid flow and geomechanics in faulted reservoirs by coupling a multiphase-flow simulator with a mechanics simulator. This two-way coupling is implemented using a fully nonlinear multiphase geomechanics formulation and an unconditionally stable iterative scheme that permits solving the flow and mechanics subproblems sequentially at each time step [Kim *et al.*, 2011, 2013; Jha and Juanes, 2014] (see supporting information). A fundamental aspect of our approach is modeling faults as surfaces of discontinuity using interface elements [Aagaard *et al.*, 2013], which permits reproducing pressure jumps across faults, as is typical of geologic faults that provide reservoir compartmentalization. This pressure jump leads to a discontinuity in the effective stress across the fault—with important consequences on forecasts of fault stability [Jha and Juanes, 2014].

We perform a dynamic simulation of the Cavone field from 1 March 1980 to 31 December 2012, imposing the historical fluid extraction and injection rates in a total of 19 wells within their actual completion intervals. We conduct the coupled simulation over the entire computational domain—even though the wells are completed within the reservoir layer (Figure 3a)—to resolve the stresses inside and outside the reservoir, and therefore account for the impact of pressure and effective stress discontinuities on the stability of the Mirandola fault. We replicate reverse faulting conditions by imposing a north-south compression as the maximum principal stress, equal to twice the lithostatic overburden stress. The Mirandola fault is assumed to act as an impermeable barrier to flow. While we cannot categorically rule out additional flow pathways, the data available show that there is no indication of flow across or along the Mirandola fault even at geologic time scales, as the fault serves as a bounding seal for the hydrocarbon reservoir. We consider a two-phase black-oil system and linear poroelastic behavior, with rock-fluid parameters that are consistent with values inferred from dedicated injection/interference well tests performed in May–June 2014, and that allow for a reasonably good history match in terms of pressure depletion and buildup (see supporting information). The reservoir pressure changes from fluid production and injection propagate down into the underlying aquifer, but the relatively small magnitude of the pressure variations is an indication of strong aquifer support (Figure 4a) (see supporting information).

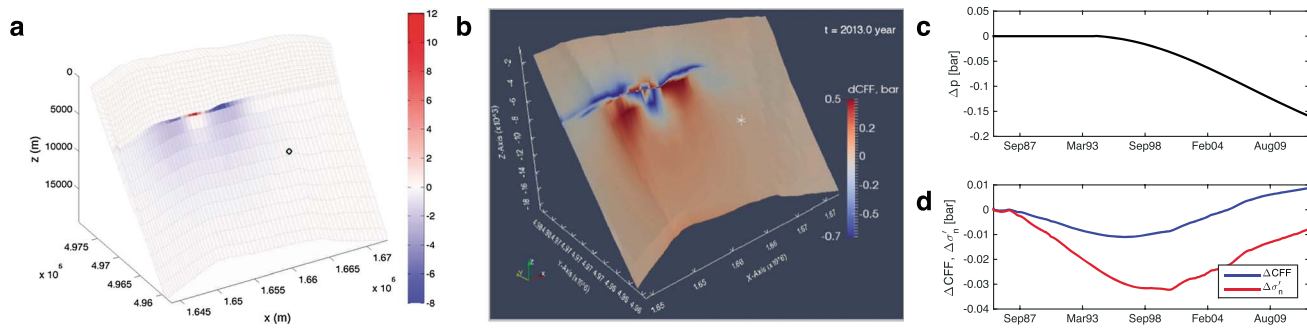


Figure 4. Results from the coupled flow-geomechanics dynamic model. (a) Pressure variation (in bar) at the hanging wall side of the Mirandola fault at the end of the simulation (31 December 2012). Red color indicates pressure buildup as a result of injection in the Cavone #14 well. Blue color indicates pressure decline as a result of fluid extraction, which extends into the underlying aquifer. The 29 May 2012 hypocenter location is shown with a circle. See Movie S1 in the supporting information for a video of the pressure-change evolution. (b) Changes in the Coulomb stress ΔCFF on the Mirandola fault (in bar) at the end of the simulation (31 December 2012). The change in the effective normal traction is positive near producers and negative near injectors because pressure depletion leads to contraction of the reservoir and pressure increase leads to increased compression on the fault. The white cross mark on the ΔCFF plot denotes the hypocenter location of the 29 May 2012 earthquake. See Movie S2 for a video of the ΔCFF evolution. (c, d) Time evolution of changes in pressure and Coulomb stress (respectively) at the 29 May 2012 hypocenter location.

Because we do not know how close a given fault segment is to failure, we cannot predict how large a stress perturbation is required to trigger an earthquake. However, we can assess the likelihood of triggering by evaluating the change in Coulomb stress, or Coulomb Failure Function, ΔCFF , on the fault as a result of changes in pressure and stress [Reasenber and Simpson, 1992; Jha and Juanes, 2014]:

$$\Delta CFF = \Delta \tau + \mu_f \Delta \sigma'_n,$$

where $\Delta \tau$ is the change in the updip shear traction, $\mu_f = 0.6$ is the fault friction coefficient, and $\Delta \sigma'_n$ is the change in effective normal traction on the fault. Because we employ the sign convention that tension is positive and compression is negative, a positive ΔCFF indicates a destabilizing effect on the fault. The region of increased instability on the (reverse) Mirandola fault is limited in spatial extent (Figure 4b), with $\Delta CFF < 0.5$ bars for reverse slip. Up to year 1994, the simulated pressure at the hypocenter of the 29 May earthquake does not change appreciably while—as a result of poroelastic expansion—the effective normal traction and the Coulomb stress both decrease. In 1995, the pressure starts to decrease, indicating that the pressure depletion front has reached the hypocenter location. Because of contraction of the aquifer from depletion, the compressive effective normal traction at the outside face of the fault starts to decrease, and, as a result, ΔCFF increases (Figures 4c and 4d).

The results from our coupled flow and geomechanics dynamic modeling shed light on possible causal mechanisms of the recorded seismicity near the Cavone oil field. Concerning the 20 May M_w 6.0 earthquake, this earthquake sourced in the Middle Ferrara fault, which is located ~ 20 km from the Cavone wells and separated from the Cavone field by two thrust sheets. Concerning the 29 May M_w 5.8 earthquake, which sourced in the Mirandola fault bounding the Cavone reservoir, a key finding from our computational modeling is that—in contrast with what is commonly observed in scenarios of induced seismicity—water injection at the Cavone #14 well tends to stabilize the fault. The explanation hinges on the coupled nature of fluid pressure and reservoir deformation. For a bounding (nonconductive) fault like the Mirandola fault, net production leads to contraction of the reservoir. This, in turn, is responsible for two kinds of stress changes. On one hand, it leads to shear stress changes in the form of downdip tractions above the reservoir and updip tractions below. On the other hand, it leads to normal stress changes: a reduction in compressive effective stress on the outside face of the Mirandola fault below the reservoir and an increase above the reservoir. The result of these effects from fluid extraction is a destabilizing stress change on the fault ($\Delta CFF > 0$) within and below the reservoir interval, an effect that is mitigated by injection that counterbalances net depletion (Figure 4b).

5. Conclusions

The results from our computational modeling study provide important elements for the interpretation of the potential role of reservoir operations on the observed seismicity in May 2012. First, the region of destabilizing

stress changes on the Mirandola fault as a result of production/injection is limited to a region that has not experienced increased seismicity during over 20 years of operation. Second, the changes in Coulomb stress in the region near the 29 May hypocenter on the Mirandola fault are, although in a sense to be destabilizing, very small (<0.02 bar), i.e., less than typical daily variations in earth tidal stresses [e.g., Vidale *et al.*, 1998] and much less than both the ~ 0.1 bar threshold for observable increased seismicity [Hardebeck *et al.*, 1998], and the estimated Coulomb stress increases of 0.2–5 bars from the 20 May event [Cesca *et al.*, 2013; Pezzo *et al.*, 2013], demonstrating very minor if any effects of production and injection at the hypocenter. The 20 May hypocenter is on a different fault and farther from the Cavone field, outside the domain of the geomechanics study, and for which the pressure changes from reservoir operations is predicted to be zero in our model. Taken together, these observations strongly suggest that the combined effects of fluid production and injection from the Cavone field were not a driver for the observed seismicity.

More generally, our study indicates that—when constrained by seismic measurements, realistic geologic representations, detailed subsurface pressure data, and other available data—computational models of coupled flow and geomechanics can inform about the origin of seismicity (whether it is induced or tectonic) and possibly help design reservoir operations that mitigate it, including, for example, injection of water to maintain mass balance.

Acknowledgments

We thank Assomineraria for permission to publish this paper. We thank Daniele Susanni, Luca Magagnini, and Fabio Colombo of Ramboll Environ Italy for facilitating data and for useful discussions. Data can be obtained from the corresponding author.

References

- Aagaard, B. T., M. G. Knepley, and C. A. Williams (2013), A domain decomposition approach to implementing fault slip in finite-element models of quasi-static and dynamic crustal deformation, *J. Geophys. Res. Solid Earth*, *118*, 3059–3079, doi:10.1002/jgrb.50217.
- Bonini, M. (2013), Fluid seepage variability across the external northern Apennines (Italy): Structural controls with seismotectonic and geodynamic implications, *Tectonophysics*, *590*, 151–174.
- Burrato, P., F. Ciucci, and G. Valensise (2003), An inventory of river anomalies in the Po Plain, northern Italy: Evidence for active blind thrust faulting, *Ann. Geophys.*, *46*(5), 865–882.
- Cesca, S., T. Braun, F. Maccaferri, L. Passarelli, E. Rivalta, and T. Dahm (2013), Source modeling of the M 5–6 Emilia-Romagna, Italy earthquakes (2012 May 20–29), *Geophys. J. Int.*, *193*, 1658–1672.
- Ciaccio, M. G., and C. Chiarabba (2002), Tomographic models and seismotectonics of the Reggio Emilia region, Italy, *Tectonophysics*, *344*, 261–276.
- Ellsworth, W. L. (2013), Injection-induced earthquakes, *Science*, *341*, 1225–1229.
- Frohlich, C. (2012), Two-year survey comparing earthquake activity and injection-well locations in the Barnett Shale, Texas, *Proc. Natl. Acad. Sci. U.S.A.*, *109*, 13,934–13,938.
- Ganas, A., Z. Roumelioti, and K. Chousianitis (2012), Static stress transfer from the May 20, 2012, M 6.1 Emilia-Romagna (northern Italy) earthquake using a co-seismic slip distribution model, *Ann. Geophys.*, *55*, 655–662.
- Guglielmi, Y., F. Cappa, J.-P. Avouac, P. Henry, and D. Elsworth (2015), Seismicity triggered by fluid injection–induced aseismic slip, *Science*, *348*, 1224–1226.
- Hardebeck, J. L., J. J. Nazareth, and E. Hauksson (1998), The static stress change triggering model: Constraints from two southern California aftershock sequences, *J. Geophys. Res.*, *103*, 427–437, doi:10.1029/98JB00573.
- Hornbach, M. J., et al. (2015), Causal factors for seismicity near Azle, Texas, *Nat. Commun.*, *6*, 6728, doi:10.1038/ncomms7728.
- Improta, L., L. Valoroso, D. Piccinini, and C. Chiarabba (2015), A detailed analysis of wastewater-induced seismicity in the Val d'Agri oil field (Italy), *Geophys. Res. Lett.*, *42*, 2682–2690, doi:10.1002/2015GL063369.
- Jha, B., and R. Juanes (2014), Coupled multiphase flow and poromechanics: A computational model of pore pressure effects on fault slip and earthquake triggering, *Water Resour. Res.*, *50*, 3776–3808, doi:10.1002/2013WR015175.
- Kawamura, H., T. Hatano, N. Kato, S. Biswas, and B. K. Chakrabarti (2012), Statistical physics of fracture, friction, and earthquakes, *Rev. Mod. Phys.*, *84*, 839–884.
- Keranen, K., M. Weingarten, G. A. Abers, B. A. Bekins, and S. Ge (2014), Sharp increase in central Oklahoma seismicity since 2008 induced by massive wastewater injection, *Science*, *345*, 448–451.
- Keranen, K. M., H. M. Savage, G. A. Abers, and E. S. Cochran (2013), Potentially induced earthquakes in Oklahoma, USA: Links between wastewater injection and the 2011 M_w 5.7 earthquake sequence, *Geology*, *41*(6), 699–702.
- Kim, J., H. A. Tchelepi, and R. Juanes (2011), Stability and convergence of sequential methods for coupled flow and geomechanics: Fixed-stress and fixed-strain splits, *Comput. Methods Appl. Mech. Eng.*, *200*, 1591–1606.
- Kim, J., H. A. Tchelepi, and R. Juanes (2013), Rigorous coupling of geomechanics and multiphase flow with strong capillarity, *Soc. Pet. Eng. J.*, *18*(6), 1123–1139.
- National Research Council (2013), *Induced Seismicity Potential in Energy Technologies*, Natl. Acad. Press, Washington, D. C.
- Pezzo, G., et al. (2013), Coseismic deformation and source modeling of the May 2012 (northern Italy) earthquakes, *Seismol. Res. Lett.*, *84*, 645–655.
- Piccinini, D., N. A. Pino, and G. Saccorotti (2012), Source complexity of the May 20, 2012 M_w 5.9, Ferrara (Italy) event, *Ann. Geophys.*, *55*, 568–573.
- Raleigh, C. B., J. H. Healy, and J. D. Bredehoeft (1976), An experiment in earthquake control at Rangely, Colorado, *Science*, *191*, 1230–1237.
- Reasenber, P. A., and R. W. Simpson (1992), Response of regional seismicity to the static stress change produced by the Loma Prieta earthquake, *Science*, *255*, 1687–1690.
- Scholz, C. H. (2002), *The Mechanics of Earthquakes and Faulting*, 2nd ed., Cambridge Univ. Press, Cambridge.
- Scognamiglio, L., et al. (2012), The 2012 Pianura Padana Emiliana seismic sequence: Locations, moment tensors and magnitudes, *Ann. Geophys.*, *55*, 549–559.
- Segall, P. (1989), Earthquakes triggered by fluid extraction, *Geology*, *17*, 942–946.

- Shaw, J. H., and J. Suppe (1996), Earthquake hazards of active blind-thrust faults under the central Los Angeles basin, California, *J. Geophys. Res.*, *101*(B4), 8623–8642, doi:10.1029/95JB03453.
- Shaw, J. H., C. Connors, and J. Suppe (2005), *Seismic Interpretation of Contractional Fault-Related Folds: An AAPG Seismic Atlas*, AAPG Stud. Geol., vol. 53, 157 pp., Am Assoc. of Petrol. Geol., Tulsa, Okla.
- Stein, R. S., and R. S. Yeats (1989), Hidden earthquakes, *Sci. Am.*, *260*(6), 48–57.
- Suppe, J., and D. A. Medwedeff (1990), Geometry and kinematics of fault-propagation folding, *Eclogae Geol. Helv.*, *83*(3), 409–454.
- van der Elst, N. J., H. M. Savage, K. M. Keranen, and G. A. Abers (2013), Enhanced remote earthquake triggering at fluid-injection sites in the midwestern United States, *Science*, *341*, 164–167.
- Vidale, J. E., D. C. Agnew, M. J. S. Johnston, and D. H. Oppenheimer (1998), Absence of earthquake correlation with earth tides: An indication of high preseismic fault stress rate, *J. Geophys. Res.*, *103*, 24,567–24,572, doi:10.1029/98JB00594.
- Weingarten, M., S. Ge, J. W. Godt, B. A. Bekins, and J. L. Rubinstein (2015), High-rate injection is associated with the increase in U.S. mid-continent seismicity, *Science*, *348*, 1336–1340.